A Novel High Birefringence Single Elliptic Photonic Quasicrystal Fiber

Qingyu Liu[1], Xiong Li[1] and Congli Wang[1,*]

[1]Noncommissioned Officer academy of PAP, Zhejiang, China

[*]Corresponding author e-mail: s_unny7723@163.com

Abstract. This A novel single elliptical photonic quasi-crystal fiber (PQF) structure based on ZrF_4-BaF_2-LaF_3-AlF_3-NaF (ZBLAN) is proposed. There is a single elliptical air hole at the fiber core and a ten-fold Person-type quasi-crystal structure distributed in the outer layer. The birefringence and confinement loss (CL) of the PQF are numerically proposed in short-wavelength infrared region (SWIR) based on finite element method. The high birefringence is achieved thanks to a single ellipse near the fiber core breaking the symmetry of the structure. Fluoride materials ZBLAN have lower CL in SWIR than traditional quartz glass. The birefringence of this novel PQF can be maintained above 10^{-2}, which will have great potential in optical devices.

Keywords: ZrF_4-BaF_2-LaF_3-AlF_3-NaF, elliptical pores, optical.

1. Introduction

PQF is based on the theoretical foundation of photonic crystal fiber (PCF) combined with quasi-crystal structures. Knight and his team drawn the first total internal reflection photonic crystal fiber in 1996 [1]. Kim et al. combined quasicrystal structure with PCF to research the optical properties of communication bands in 2007 [2]. The change in PQF air holes can achieve unexpectedly superior optical properties such as high birefringence [3-6], nonlinearity [7], large mode field area [8], and near zero dispersion [9]. PQF can have important applications in sensors [10], nonlinear optics [7], rotational angular momentum communication systems [11] and other fields [12].

In recent years, research on HB-PQF background materials has expanded many new materials [13], which is no longer limited to silica. ZBLAN is a heavy metal fluoride (HMF) material that has been widely studied due to its easy to draw properties and lower absorptivity than silica around communication band range.

Herein, we describe a birefringence PQF with a single elliptical air hole in the core to improve the asymmetry and achieve high birefringence (on the order of 10^{-2}), and the outer array of Person-type ten-fold lattice structures to reduce CL (on the order of 10^{-2}) in the SWIR.

2. Structure and theory

Figure 1. cross section of novel PQF based on ZBLAN glass. PQF with a single elliptical air hole in the right of core and the outer array of Person-type ten-fold lattice structures. The PQF structure is divided into four layers from the fiber core to the outer layer. The circular air holes from the first layer to the fourth layer are labeled in pink, blue, yellow, and green colors, and their diameters are labeled as d_{1st}, d_{2nd}, d_{3rd}, and d_{4th}. Among them, the second layer has two deep blue air holes located on the horizontal axis, with a diameter of $d_{2nd\text{-}2}$. The major axis and minor axis of the ellipse near the fiber core are a and b, respectively. The design of basic quasicrystal units is to effectively confine light within the fiber core. It can be demonstrated through experiments that adding an elliptical hole at the core of the fiber structure can improve birefringence and also achieve single-mode transmission

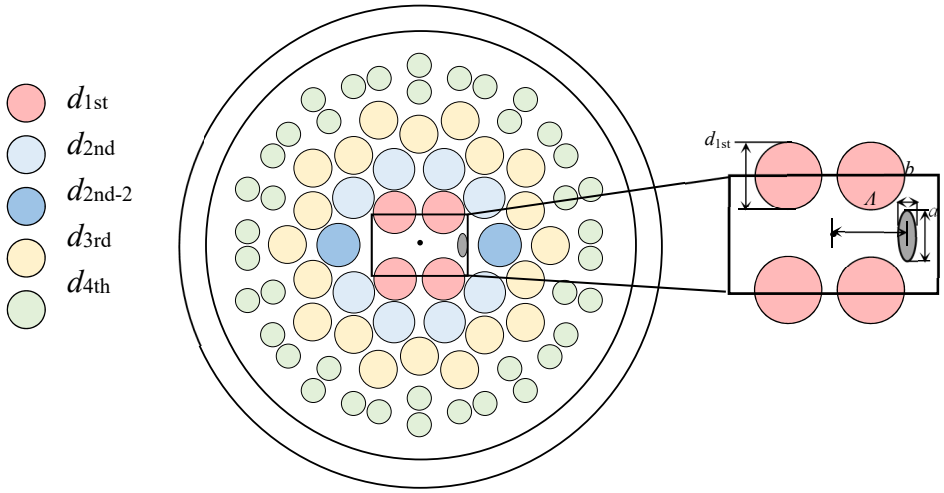

Figure 1. Cross section of novel PQF based on ZBLAN glass.

The effective indexes for different modes are calculated based on perfectly matched layer boundary conditions and using the full vector finite element method(FEM). The refractive index is calculated based on the Sellmeier equation, and the refractive index of ZBLAN fiber is represented as follows:

$$n_\lambda^2 - 1 = \frac{f_1\lambda^2}{(\lambda^2-\lambda_1^2)} + \frac{f_2\lambda^2}{(\lambda^2-\lambda_2^2)} \tag{1}$$

where λ_1 and λ_2 are the intrinsic absorption wavelength of ultraviolet and infrared, f_1 and f_2 stand for oscillator strength of ultraviolet and infrared, respectively. In the ZBLAN fiber λ_1, λ_2, f_1, and f_2 are 0.08969 μm, 21.3825 μm, 1.22514, and 1.52898, respectively [14].

The formula for expressing birefringence is as follows:

$$B = \lambda\frac{\beta_x-\beta_y}{2\pi} = n_{\text{eff}}^x - n_{\text{eff}}^y \tag{2}$$

where n_{eff}^x,n_{eff}^y represent the effective refractive indexes in the polarization directions of x and y [13].

The calculation of CL is mainly based on the imaginary part of the effective refractive index of the fundamental mode, which reflects the constraint ability of the core region [16].

$$CL = \frac{20}{ln\,10} Im(\beta) = \frac{20}{ln\,10} k_0 Im(n_{\text{eff}}) \tag{3}$$

where *Im* represents the imaginary part of the effective refractive index, k_0(k_0=2 π/ λ) is the free space wavenumber.

The loss characteristics of PQF are not researched separately and are often complementary to characteristics such as birefringence or high nonlinearity. In practical applications, as CL directly affects the efficiency of optical fibers, it is necessary to calculate loss while measuring other optical characteristics.

3. Results and Discussion

The structural parameters of PQF are changed to achieve both high birefringence and low CL. The initial value used for the photonic quasicrystal fiber structure are d_{1st} = 1.6 μm, d_{2nd} = d_{2nd-2} = 1.55 μm, d_{3rd} = 1.4 μm, d_{4th} = 0.85 μm, ρ = b/a = 1/0.4, Λ = 1.5 μm. This article researches the optical properties when certain parameters (d_{1st}, d_{2nd}, ρ, Λ) are changed.

3.1 The influence of the diameter of circular air holes.

Figure 2 shows the calculated variation curve of birefringence when the d_{1st} range is changed from 1.45 to 1.6 μm and other parameters are fixed. Birefringence increases with the increase of wavelength, which is caused by the increase in effective refractive index difference of the two orthogonal polarization modes. When d_{1st} increases, birefringence also increases significantly. Due to the increase in air holes, the squeezing of the core mold field also increases, which effectively binds the beam to the core. However, when the diameter of d_{1st} increased to 1.55 μm, the amplitude of change rapidly decreased. The numerical difference of birefringence between the sizes 1.55 μm and 1.6 μm is on the order of 10^{-3}, and the birefringence curves almost overlap. The d_{1st} at 1.55 μm is the ideal maximum value for simulation, and exceeding this value during actual manufacturing can cause the d_{1st} air holes to fuse with other air holes.

When the d_{1st} are fixed at 1.55 μm, the d_{2nd-2} is changed from 1.45 to 1.55 μm. The simulated birefringence is shown in Figure 3 Birefringence increases with the increase of d_{2nd-2} and wavelength.

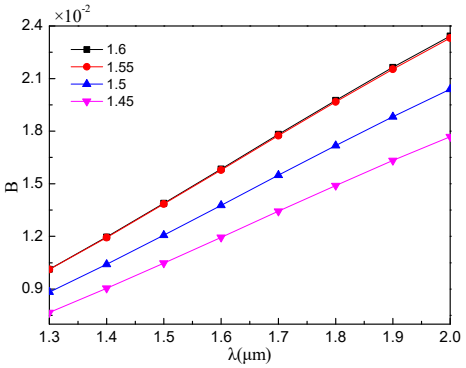

Figure 2. Birefringence for different d_{1st}

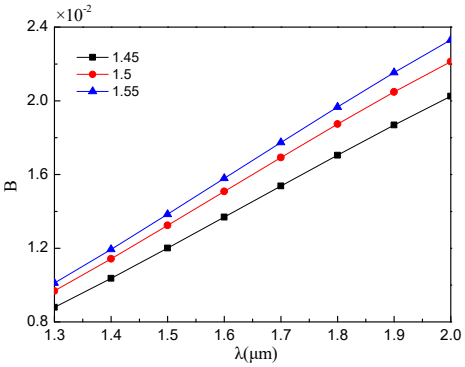

Figure 3. Birefringence for different d_{2nd-2}

Figure 4 shows that as d_{1st} increases, the CL in both x and y polarization directions also increase exponentially. The CL changes of different d_{2nd-2} shown in Figure 5 are similar to Figure 4. The single elliptical air hole at the fiber core results in higher CL in the x direction than in the y direction. Because the elliptical air hole is on the horizontal axis, its effect on the mode field in the x direction is stronger than that in the y direction. Here, d_{1st} = 1.55 μm, d_{2nd-2} = 1.55 μm are selected as the optimal value considering birefringence, CL, and actual size.

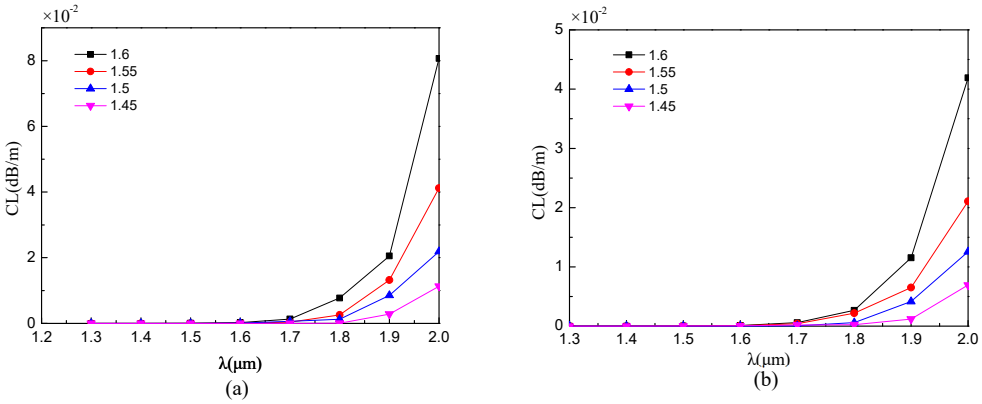

Figure 4. CL for different d_{1st} in (a) x-polarized mode, (b) y-polarized mode

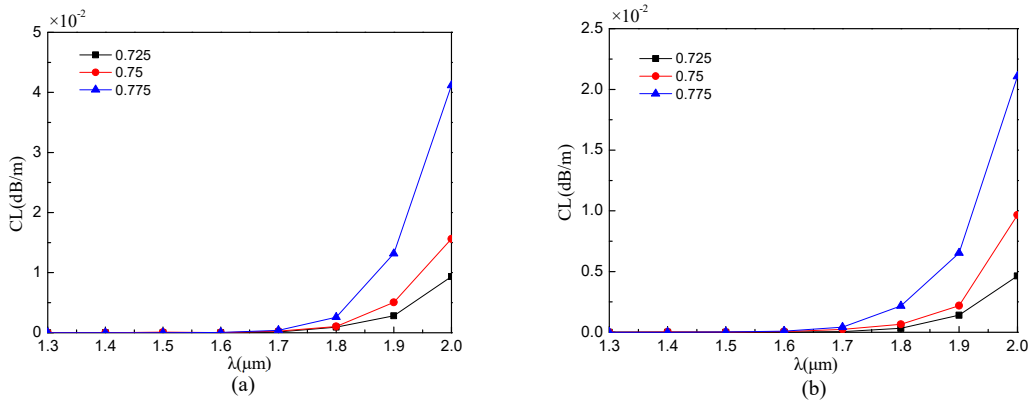

Figure 5. CL for different d_{2nd-2} in (a) x-polarized mode, (b) y-polarized mode

3.2 The influence of the diameter of circular air holes.

Figure 6 shows the change in birefringence when the ellipticity ρ changes. The influence of the long axis on the symmetry of the structure is more pronounced. Therefore, increasing the long axis will more effectively improve birefringence than increasing the short axis. Figure 6(a) shows that the six curves almost overlap. Figure 6(b) shows subtle differences within the range of 1.5 — 1.7μm. When ρ=1.0/0.44, the birefringence value in this band reaches 1.799×10^{2}.

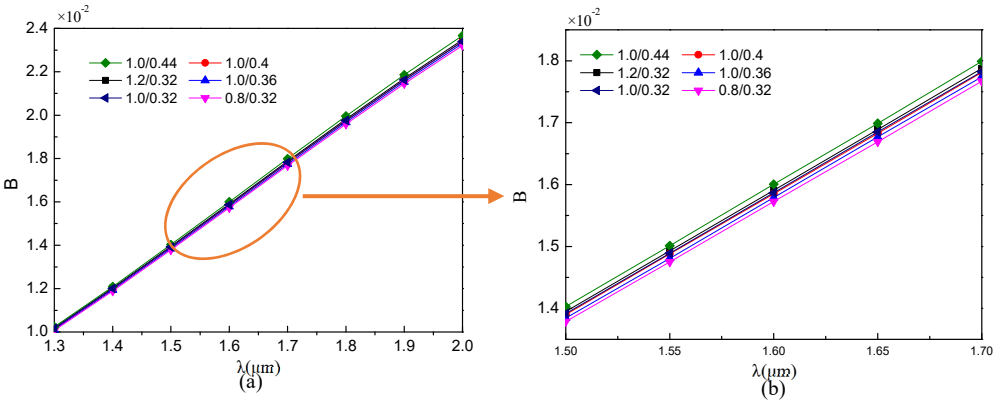

Figure 6. Birefringence for different ρ in the wavelength range of (a)1.3 — 2μm, (b) 1.5 — 1.7 μm

As shown in Figure 7, the CL is influenced by the ellipticity, and the CL in the x-polarization direction is significantly higher than that in the y-polarization direction. When the short axis increases excessively, it will cause the x-polarization direction loss to be effectively cut off, and only the y-polarization direction mode is transmitted in the fiber core. Therefore, after six sets of ellipticity (ρ = 0.8/0.32, ρ = 1.0/0.32, ρ = 1.2/0.32, ρ = 1.0/0.36, ρ = 1.0/0.4, ρ = 1.0/0.44) comparison experiments and analysis, the high birefringence parameter is ρ = 1.0/0.44.

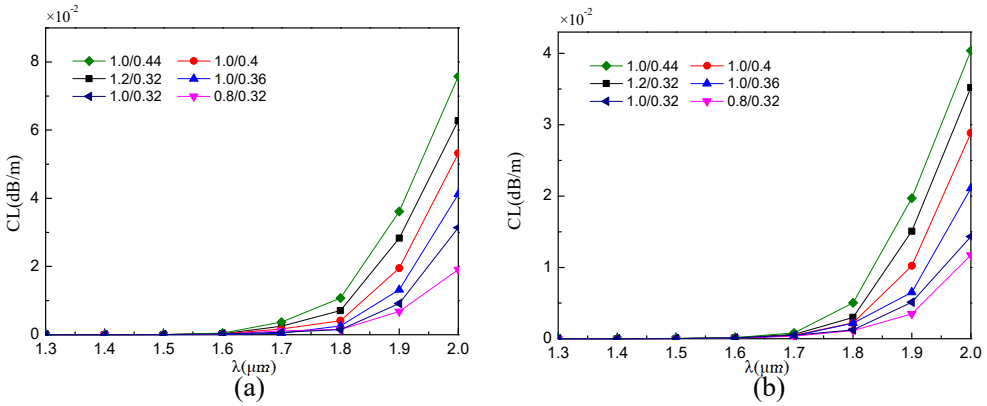

Figure 7. CL for different ρ in (a) x-polarized mode, (b) y-polarized mode

3.3 The influence of elliptical position Λ.

The final parameter to change is the position of the ellipse from the center of the circle Λ. The comparison of birefringence under three sets of parameters（1.3 μm, 1.5μm, 1.7 μm）is shown in Figure 8. The elliptical air hole at the fiber core causes compression of the fiber core area, which enhances the interaction between the elliptical air hole and the fiber core mode field, thereby increasing birefringence. High birefringence is accompanied by a smaller λ, and the elliptical air hole coincides with d1 on the upper right when λ is too small. The final selected structural parameter are $d_{1st} = d_{2nd\text{-}2} = 1.55$μm, $\rho = 1.0/0.44$, Λ=1.3μm with birefringence reaching 2.47×10^{-2} at 2μm, and loss in both polarization directions not exceeding 0.01dB/m.

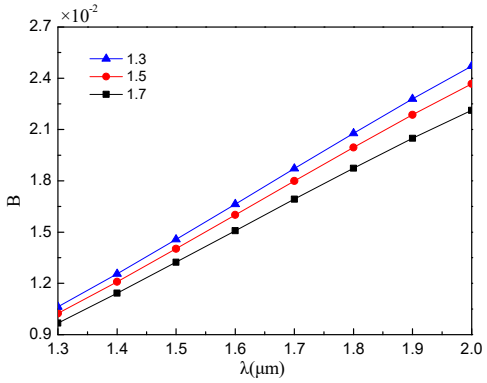

Figure 8. Birefringence for different Λ

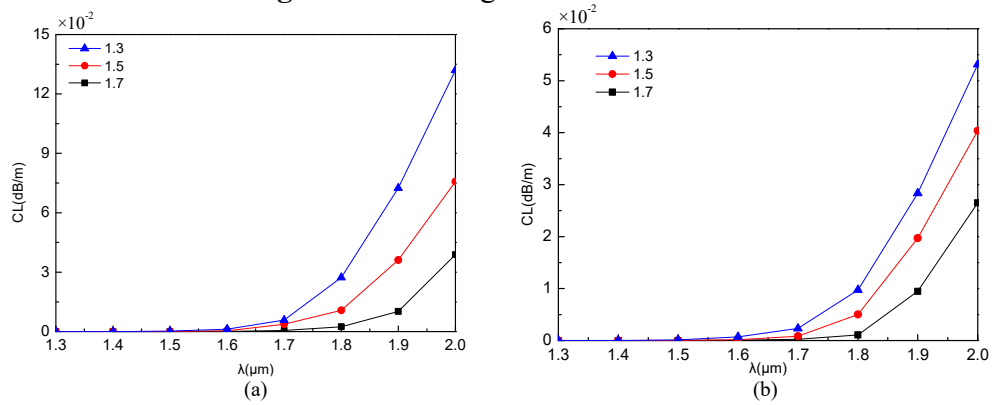

Figure 9. CL for different ρ in (a) x-polarized mode, (b) y-polarized mode

Figure 10 shows the mode field distribution of the PQF structure at an incident wavelength of 1.5 μm. Due to the addition of a single elliptical air hole, the light confinement effect in the x and y polarization directions also varies.

4. Conclusion

This article describes a single elliptical ten-fold PQF with a background material of ZBLAN high birefringence and low loss. Ultimately, the birefringence can reach 10^{-2} in the communication and eye safety bands, which is superior to traditional optical fibers after parameter optimization iterations.

References

[1] J.C. Knight, T.A. Birks, P.St.J. Russell, and D.M. Atkin, All-silica single-mode optical fiber with photonic crystal cladding, Opt. Lett. 21 (1996) 1547-1549.

[2] S.Kim, C.S. Kee and J. Lee, Novel optical properties of six-fold symmetric photonic quasicrystal fibers, Opt. Express, 15 (2007) 13221-13226.

[3] H. Liu, W. Xiao, W. Cai, et al: Photonic quasi-crystal fiber with high birefringence, Opt. Eng. 55 (2016) 036101.

[4] W. Cai, E. Liu, B. Feng, et al. Dodecagonal photonic quasi-crystal fiber with high birefringence, J. Opt. Soc. Am. A, 33 (2016) 2108-2114.

[5] Q. Liu, Q.Y. Liu, Y. Sun, et al, A high-birefringent photonic quasi-crystal fiber with two elliptical air holes, Optik, 184 (2019) 10-15.

[6] Q. Liu, Z. Ren, Y. Sun, et al, Numerical analysis of a high-birefringent photonic quasi-crystal fiber with circular air holes, Optik, 207 (2020) 163850.

[7] T. Zhao, S. Lou, W. Su, et al. Design of an As2Se3-based photonic quasi-crystal fiber with highly nonlinear and dual zero-dispersion wavelengths, J. Mod. Optic. 63 (2015) 1-7.

[8] E. Liu, W. Tan, B. Yan, et al. Broadband ultra-flattened dispersion, ultra-low confinement loss and large effective mode area in an octagonal photonic quasi-crystal fiber, J. Opti. Soc. Am. A, 35 (2018) 431-436.

[9] E. Liu, B. Yan, W. Tan, et al. Guiding characteristics of sunflower-type fiber, Superlattice. Microst. 115 (2018) 123-129.

[10] Q. Liu, J. Sun, Y. Sun, et al. Surface plasmon resonance sensor based on eccentric core photonic quasi-crystal fiber with indium tin oxide, Appl. Optics, 58 (2019) 6848-6853.

[11] Q. Liu, S. Tai, Y. Sun, et al. A photonic quasi-crystal fibre supporting stable transmission of 150 OAM modes with high mode quality and flat dispersion, J. Mod. Optic. 69 (2022) 887-896.

[12] S. Sivabalan, J.P. Raina: Large Pitch Photonic Quasi-Crystal Fiber Amplifier, IEEE Photonics J. 4 (2012) 943-951.

[13] M. Valliammai, S. Sivabalan, Wide-band supercontinuum generation in mid-IR using polarization maintaining chalcogenide photonic quasi-crystal fiber, Appl. Optics, 56 (2017) 4797-4806.

[14] F. Gan, Optical properties of fluoride glasses: a review, J. Non-Cryst. Solids, 184 (1995) 9-20.

[15] J.C. Knight, T.A. Birks, P.S.J. Russell, J.P.D. Sandro: Properties of photonic crystal fiber and the effective index model, J. Opt. Soc. Am. 15 (1998) 748-752.